Date of publication JUN-30, 2025, date of current version APR-15, 2025.
www.computingonline.net / computing@computingonline.net

Print ISSN 1727-6209
Online ISSN 2312-5381
DOI 10.47839/ijc.24.2.4022

An Efficient Transfer Learning Hybrid Model for Multiclass Brain Tumor Classification

NEELAM KHEMARIYA, SUMIT SINGH SONKER, JAVED WASIM
Mangalayatan University, Aligarh, Uttar Pradesh, India

Corresponding author: Neelam Khemariya (neelam.khemariya@gmail.com).

ABSTRACT Brain tumors are the most dangerous diseases today. Brain tumors have come second among the diseases that cause the most deaths in the world. Conventional techniques used to diagnose brain tumors are time-consuming and prone to error. Transfer learning algorithms have also been used to detect brain tumors and are still being used extensively. After studying the previous research paper, we found two shortcomings. First of all, in most of the work, researchers modified a particular Convolutional Neural Network, which found only the features of that Convolutional Neural Network, and the second one mostly worked on a single-class detection, which means that the model will detect whether the given input image is tumorous or not. However, these models are not able to identify the multiclass tumors. Keeping both these things in mind, in this research paper, we have introduced a hybrid multilabel classifier model in which ResNetV2 and EfficientNetV2B3 have been combined to get their best features with ImageNet weights. Combining ResNetV2 (the best Residual Convolutional Network for multilayer and multiclass classification) and EfficientNetV2B3 (the best Convolutional network for faster calculation) helped us to deploy a faster multilayered classifier model. The last 30 layers of both have been trained accordingly, and 16 custom layers have been included. The dataset contains 3 types of tumor images (glioma, meningioma, and pituitary) and non-tumor images. The model was trained with 4569 human Brain MRI images and then validated with 1143 images. The model was tested on 1311 images, and its performance was measured for multiclass tumors. The overall accuracy of the presented model was measured at 100% during training and 99.1% during testing, which shows that our model works very accurately. As a multiclass classifier, it achieved maximum accuracy value, maximum recall value, maximum precision value, and maximum F-1 score value of 99.1% (all classes), 100.00% (Pituitary and No tumor classes), 100.00% (No Tumor class), and 100.00% (No Tumor Class), respectively.

KEYWORDS Brain Tumor; Transfer Learning; Residual CNN; EfficientNetV2B3; ResNetV2; Multiclass Tumor; Confusion Matrix; Accuracy; CLAHE.

I. INTRODUCTION

The advancement of Machine Learning tools and the accurate prediction of huge data values in just a few seconds made the routine of human beings more comfortable. The advanced techniques of artificial intelligence have made every area of human life, like houses, entertainment, safety, comfort, health, education [1], and daily life very convenient [2]. Apart from this, they are playing an important role in many areas like the stock market, business, education, medical, robotics, hotels, etc. Very good work on machine learning usability and applicability in the diagnosis of many medical diseases is shown in [3] These advanced techniques have completely cured many dangerous diseases in the medical field like heart disease [4], diabetes [5], pancreatic cancer [6], coronavirus [7], Breast cancer [8], skin cancer [9] and many more, and are playing a huge role in many of these problems. Brain tumor is a type of disease that starts due to unnecessary or uncontrolled growth of tissues in the brain of a human being, and if it is not controlled or eliminated properly by this age, it can take the form of a terrible brain cancer. It is difficult to control it, especially if it is found out in the last stage. The World Health Organization has classified brain tumors into 4 grades after observing their presentation, in which lower-grade tumors are considered non-dangerous and curable, but high-grade tumors are considered cancerous and are very difficult to cure [10]. Identifying a brain tumor using basic medical techniques and making its timely diagnosis is a matter of concern, and the possibility of error in its measurement cannot

be ruled out. Keeping all these issues in mind, we have presented a very innovative and refined technique based on faster models and the superiority of transfer learning, which can classify and evaluate brain tumors efficiently, with very low error chances. The present research is specifically designed to classify and identify three types of brain tumors: glioma tumor, meningioma tumor, and pituitary tumor. Glioma tumors are cancerous and they belong to the group of malignant tumors, which is why they are difficult to cure. Meningioma tumors are included in the group of benign tumors, hence, the chances of curing them are very high. Pituitary tumors are a group of benign tumors and are not dangerous, so the chances of curing them are very high.

II. BRAIN TUMOR BASICS

Any undesirable widening inside the tissues of the brain is designated as a tumor in the brain. Every type of tumor in the brain comes under the category of brain contusion. However, every contusion in the brain is not necessarily a tumor in the brain [11]. A specific type of contusion in a particular damaged tissue of the brain area is known as a brain lesion. It is not always true that a tumor in the brain is cancerous or further after a long time it can be converted into cancer. Due to its origin, a Brain tumor can be further categorized in two ways – primary (origin is brain) or metastatic (origin is any part of the body other than the brain. Tumors originating from the tissues inside the brain can be further subcategorized as cancerous, designated as Malignant, or non-cancerous, designated as Benign. Cancerous and non-cancerous tumors of the brain have a long taxonomy, described and classified based on their effect, range, possibility, symptoms, age range, vulnerability label, cure, and many more factors. As per the fatality level of these tumors, the WHO designated them into four categories – Grade I, II, III, and IV. Grade I category tumors have a fatality level of 0 or much less, while Grade IV category tumors have the highest fatality level, and they are 99.9% cancerous [12].

Some common symptoms can be spasms, expatriating, headache, numbness, immobility, reeling, unsteadiness, modification to sight, variation in views, insensibility, perplexity, fugue, or dullness [13]. Although the causes are unknown, some possible reasons causing the tumor may be obesity, stoutness, no history of herpes varicella, a person getting older, genetic, or different dangerous birth syndromes, radioactivity, Neurological disorders, or some other kind of cancer. The diagnosis initially passes through some neurological observations, including basic tests such as blood tests or neurological examinations. Further detailed examination can be done through CT scan, Brain MR imaging techniques, or Endomicroscopy [14]. If the results of the diagnosis are positive, then Treatment needs to be started immediately, so that it can be cured in the early stage. Some possible initial level treatments include surgical procedures and high-capacity X-ray radiation, while later-stage treatments can be achieved via Chemotherapy or advanced Laser Interstitial Thermal therapy.

III. PREVIOUS WORK

In [15], a new technique, merging threshold and region-based segmentation with the convolutional neural network, by which tumor and non-tumor areas can be distinguished very easily. Some advanced pre-processing imaging techniques have been used to make this technique even more effective. To prove the applicability of this work, a meaningful performance benchmark, Dice coefficient, has been used, whose values are 57% for CNN, and 87.8% for region-based segmentation, while the highest measured is 99% for threshold-based segmentation. [16] defined a new technique combining two-dimensional U-Net and YOLOv5 and applied it to BTF datasets, which is very effective in identifying different types of tumors and figuring out the affected area. The BRATS2018 datasets have been utilized here to specifically identify glioma tumors and have been fine-tuned before use to achieve more accurate results. In [17], A new method is presented that includes a mini-batch K-means approach with K-means approach for effective and faster tumor segmentation. By applying some special operations such as dilation, erosion, denoising, and linear transformations on the images present in the dataset, the dataset has been made more capable of getting more accurate results. An Investigation of brain tumors by different types of tissue classes is done in [18], covering the various types of tumors with their gradings. The model made 87% accurate predictions in detecting the type of tumor, 97% in terms of tumor grading, 86% in terms of glioma margin, while a 91% accurate prediction was made for IDH mutation. The Authors in [19] have developed an attention-based U-shaped CNN using the BRATS2021 datasets, whose complexity is much less than previously available models. In the Dice score benchmark, the model scores 91%, 93%, and 94% for enhancing tumor, core tumor, and whole tumor, respectively. A very dangerous brain tumor occurring in children is called glioblastoma, which can even lead to death if not treated in time. A technique based on the self-organizing map has been proposed in [20]. To increase the effectiveness of the model, maximum and minimum image rationalization techniques have also been added. The model has been successful in achieving an accuracy of 98%. An approach has been presented using Global Transformer Networks [21], covering the detailed information of the tumor to detect smaller or larger lesions. The dense layer of neurons shaped like a few English letters and responsible for forming new memories is known as the Hippocampus. Sometimes during the treatment of brain tumors, radiation can also affect the Hippocampus, which can cause the person to remember things, learn, and remember the path, orientation, or location. In [22], an AI-based encoder-decoder architecture has been used, which works in the post-operative region and resolves the issue of the Hippocampus. If the brain tumor is detected in its early stages, the chances of saving a person's life by treating it are very high. Keeping this in mind, a T-shaped biosensor has been designed in [23] by considering a new material approach in which silver, gold, and bismuth are used as resonators and machine learning techniques as executors. In [24], the authors have developed the ResUNet++ 3D model using the BRATS2019, BRATS 2020, and BRATS 2021 datasets. The ResNet50 is used as an encoder, while Convolutional Transpose layers are used as a decoder. The model can detect both high-grade and low-grade gliomas. Notable work was achieved in [25] using DconV Transformers and multilayer attenuation to achieve the accuracy of the correct prediction as 98.63%. Authors in [26] use a combination of VGG 19, Inceptionnetv3, and mobilenetv2 to achieve an accuracy of effective classification of 98.58%. Authors in [27] use SVM for effective classification while achieving only 96% prediction accuracy, 96% of the F1-score, and a recall parameter of 96%. Authors in [28] use KNN and Mask R-CNN and achieved 96% prediction accuracy, 93% of the F1-score, and a recall parameter of 93%.

IV. MATERIAL AND METHODS

Here, we have presented the methodology of the suggested work. The proposed work contains the approach for segmentation and categorization of brain tumors deployed on the MRI brain dataset using the transfer learning approach. The suggested flow of the model is shown in Figure 1 below:

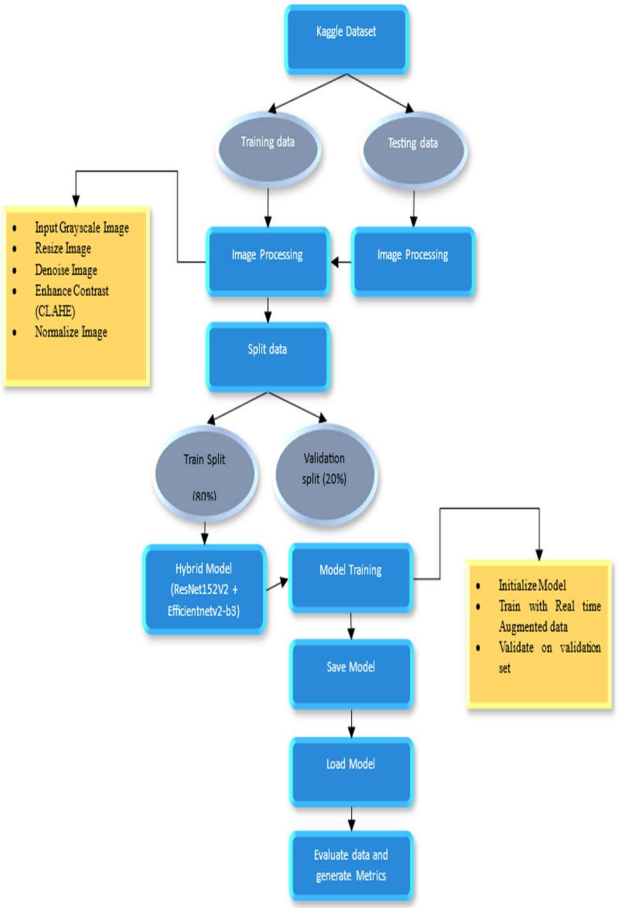

Figure 1. Flow of the Proposed Approach.

A. DATA COLLECTION

The dataset considered here is a freely available public dataset. This dataset is the fusion of three well-known public datasets – Br35H, Figshare, and SARTAJ. The dataset contains 7023 samples of human Brain MR Imaging. In 7023 images are initially classified into two types of samples – first training data samples and second testing data samples. This dataset includes 4 types of images which 3 types of images are tumor images (pituitary tumor, glioma tumor, and meningioma tumor), and the remaining images represent no tumor images. In the training sample, there were 1457 images of pituitary tumors, 1321 images of glioma tumors, 1339 images of meningioma tumors, and 1595 images of healthy means no tumor (total 5712). Similarly, in testing sample data, there were 300 images of pituitary tumor, 300 images of glioma tumor, 306 images of meningioma tumor, and the remaining 405 images of no tumor (total of 1311). Because there were no image samples for validation in the dataset, we divided the original training samples into two parts. The first part contains the training samples, which contain 80% of the images of the first training sample (total of 4569 images), which are used for training, and the second part contains the validation samples, which contain 20% of the images (total 1143 images) which he used for validation. Figure 2 represents this new reshaping of datasets.

Total Samples (Images)	Training (Samples) 4569	No Tumor 1286	Pituitary Tumor 1158	Glioma Tumor 1033	Meningioma Tumor 1092
	Validation (Samples) 1143	No Tumor 319	Pituitary Tumor 265	Glioma Tumor 268	Meningioma Tumor 291
7023	Testing (Samples)	No Tumor	Pituitary Tumor	Glioma Tumor	Meningioma Tumor
	1311	405	300	300	306

Figure 2. Dataset used for Testing and Training.

B. IMPROVEMENT USING PRE-PROCESSING TECHNIQUES

We have 4 classes whose labels represent glioma tumor, meningioma tumor, pituitary tumor, and no tumor. For experimental analysis, we have taken an input image size of 224, processed in 100 epochs with a batch size of 10. We have divided the training image dataset into two parts in the ratio of 80% and 20%, in which the first part is used for training and the second part is used for validation. It is believed that medical analysis, especially of brain tumors, can be done better on grayscale images, so we have converted the images in our dataset into grayscale images. All these images were collected from different sources, so we have resized the images so that images appear to be of the same size. In Figure 3 below, we have shown a sample of grayscale images of all 4 types of classes.

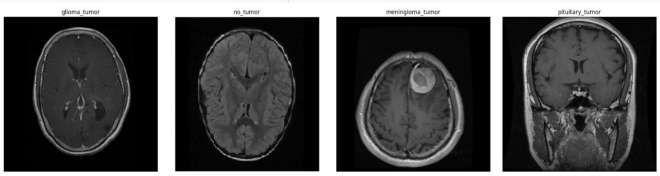

Figure 3. Representation of Grayscale Images Before CLAHE.

We used some image quality enhancement pre-processing techniques here. We removed noise from images (image denoising) because noisy images can also be responsible for wrong predictions. For image denoising, we used the fastNlMeansDenoisingColored method. To enhance the contrast, a very popular equalization technique, Contrast-limited adaptive histogram equalization, also known as CLAHE for short, has been used. two important parameters, clipLimit and titleGridSize used in CLAHE. clipLimit is used to set the threshold value of the contrast limit, while titleGridSize is used to set the number of titles in a row and column. Finally, we normalized these images. The normalization can be achieved by putting the range of these images between 0 and 1, by dividing every image by 255, separately, because the grayscale images lie in the range of 0 to 255. Figure 4 shows the Representation of Grayscale Brain MRI Images after applying CLAHE.

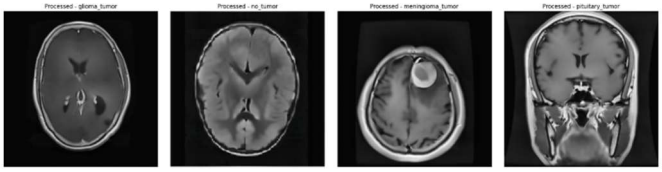

Figure 4. Representation of Grayscale Images After CLAHE.

C. FORMATION OF MODEL

To achieve a level of prediction and accurate classification in the brain tumor task, we have utilized two convolutional neural networks as a base network and derived a hybrid model from them. The reason behind taking 2 convolutional neural networks is to utilize the best features of both models and create a better model that is very effective and has a low probability of error. The first CNN we have taken is EfficientNetV2B3, which is a faster convolutional neural network. It has 384 layers and is used for faster and more accurate processing. More information on EfficientNetV2 can be obtained from [29]. The second model we took is ResNetV2, which has 564 layers and is a residual neural network used to access deep features [30]. To prepare the hybrid model, we have fine-tuned the last 30 layers of both CNNs and then added 16 custom layers, which contain 1 input layer, 6 dense layers, 6 dropout layers, 1 output layer, and 2 Conv Layers, to enhance the performance of the model. To build the hybrid model, we have used EfficientNetV2B3 and ResNet152V2. For this, initially, we have connected the inputs from both these CNNS and applied a global averaging pooling layer on the output obtained from this, so that by computing the average value of all channels, every channel can be mapped to a single value. And after this, we have applied Dense Layer, Batch Normalization, Activation, and dropout layers, respectively, repeatedly on the output obtained so that our model can be ready as per our requirement. The weights are adjusted from ImageNet due to its prompt performance [31]. The schematic diagram of our model is shown in Figure 5.

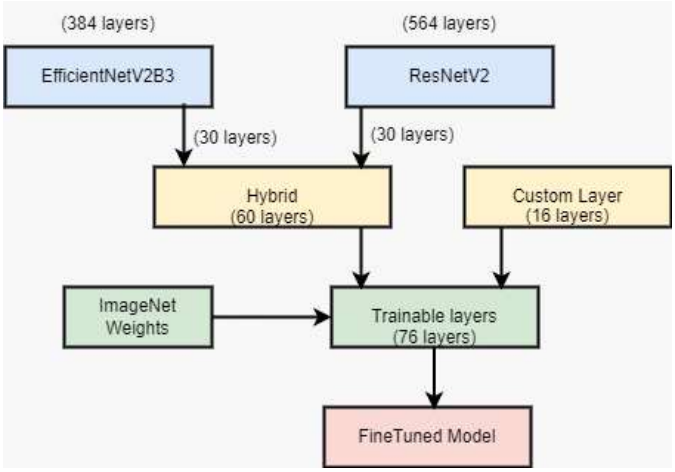

Figure 5. Schematic Diagram of the Proposed Hybrid Model.

Initially, we apply batch normalization, which is used to normalize the images by applying the RELU [48]. We applied the SoftMax activation function on the FCC layer for prediction and classification purposes. The entire process of fine-tuning our base model, a hybrid model, has been prepared, and its summary is shown in Fig. 6. This model requires 444.51 MB of memory to load 116,525,108 parameters. The trainable parameters are 20,463,736, and 78.06 memory is used to load them. Non-trainable parameters are 55,133,898, which used 210.32MB of memory to load. Additionally, it has 156.13 MB of memory to load 40,927,474 optimizer parameters.

Layer (type)	Output Shape	Param #	Connected to
input_layer_51 (InputLayer)	(None, 224, 224, 3)	0	-
efficientnetv2-b3 (Functional)	(None, 7, 7, 1536)	12,930,622	input_layer_51[0][0]
resnet152v2 (Functional)	(None, 7, 7, 2048)	58,331,648	input_layer_51[0][0]
global_average_pooling2d… (GlobalAveragePooling2D)	(None, 1536)	0	efficientnetv2-b3[0][…
global_average_pooling2d… (GlobalAveragePooling2D)	(None, 2048)	0	resnet152v2[0][0]
concatenate_10 (Concatenate)	(None, 3584)	0	global_average_poolin… global_average_poolin…
dense_40 (Dense)	(None, 1024)	3,671,040	concatenate_10[0][0]
batch_normalization_30 (BatchNormalization)	(None, 1024)	4,096	dense_40[0][0]
activation_70 (Activation)	(None, 1024)	0	batch_normalization_3…
dropout_38 (Dropout)	(None, 1024)	0	activation_70[0][0]
dense_41 (Dense)	(None, 512)	524,800	dropout_38[0][0]
batch_normalization_31 (BatchNormalization)	(None, 512)	2,048	dense_41[0][0]
activation_71 (Activation)	(None, 512)	0	batch_normalization_3…
dropout_39 (Dropout)	(None, 512)	0	activation_71[0][0]
dense_42 (Dense)	(None, 256)	131,328	dropout_39[0][0]
batch_normalization_32 (BatchNormalization)	(None, 256)	1,024	dense_42[0][0]
activation_72 (Activation)	(None, 256)	0	batch_normalization_3…
dropout_40 (Dropout)	(None, 256)	0	activation_72[0][0]
dense_43 (Dense)	(None, 4)	1,028	dropout_40[0][0]

Total params: 116,525,108 (444.51 MB)
Trainable params: 20,463,736 (78.06 MB)
Non-trainable params: 55,133,898 (210.32 MB)
Optimizer params: 40,927,474 (156.13 MB)

Figure 6. Summary of the Hybrid Model.

D. MODEL OPTIMIZATION AND AUGMENTATION

A popular optimizer, Adam, is used for optimization purposes, with a learning rate of $1e^{-4}$, and the loss value is calculated using a popular loss function, i.e., categorical cross-entropy. Input is passed in batches of 10 for effective processing, for a total number of 100 epochs. The accuracy is obtained by setting the effective Accuracy matrix. Optimization parameters are required for the optimization and performance enhancement of the model [32]. Optimization parameters and their adapted values are shown in Figure 7. The number of samples increased by applying augmentation techniques to the dataset. To make our model more effective, we applied these augmentation techniques randomly [33]. The augmentation is achieved by various techniques such as limited rotation of 20 degrees, a slide shift of 0.2 in width and height, zooming by 20 percent, distorting the image by 20 percent using shear transformation, and taking the background as black by setting fill mode as constant. Augmentation techniques adapted and their values taken are shown in Figure 8.

Parameter	Value
Loss	Categorical Crossentropy
Optimizer	Adam
Learning rate	1e-4
Metrics	accuracy
Batch Size	10
Epochs	100
Normalization	Yes

Figure 7. Summary of Optimizer Parameters.

Parameter	Value	Remark
Rotation	20	Rotation for Medical Images
Width Shift	0.2	Shift in Width
Height Shift	0.2	Shift in Height
Fill mode	Constant	Black Background
Zoom	0.2	Zooming Image
Horizontal Flip	True	MRI's can be flipped horizontally
Shear	0.2	Distorting Image
cVal	0	Fill Value

Figure 8. Summary of Data Augmentation Parameters.

Figure 9 shows the effect of data augmentation methods – Rotation, Width Shift, Height shift, Shear, and Zoom applied on grayscale images.

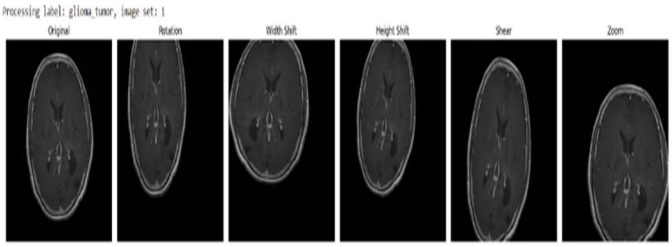

Figure 9. Effect of Data Augmentation on Grayscale Images.

V. TRAINING AND TESTING

A. TRAINING PHASE

To perform our experiments, we used Google Colab Pro +, which processes very fast due to its background processing capability and is capable of giving results very quickly. For this, we used NVIDIA's Tesla T4 GPU, which is commonly known as the T4 GPU. The use of 25 GB capacity RAM helped in completing this experiment even faster. The total time taken to maintain the model was 6318.80 seconds, while the initial and final system memory usage statuses were 28784.277 MB and 35360.9765 MB in sequence.

The Proposed model is trained using a Batch size = 10 and an epoch size = 100. The validation of training is achieved through a confusion matrix, which is based on True Positive, False Positive, True Negative, and False Negative [34]. Benchmarks considered for performance are Accuracy, F1 Score, Recall, Precision, Weighted Average, and Macro Average [35]. The performance of the model, using the following formulae:

$$Accuracy = \frac{TN + TP}{TN + FN + TP + FP}, \quad (1)$$

$$Precision = \frac{TP}{TP + FP}, \quad (2)$$

$$Recall\ (TPR) = \frac{TP}{(TP + FN)}, \quad (3)$$

$$F1 - Score\ = 2 * \frac{PPV * TPR}{PPV + TPR}, \quad (4)$$

$$Specificity\ (TNR) = \frac{TN}{TN + FP}. \quad (5)$$

In Figure 10, we have displayed the confusion matrix of training. The confusion matrix is generated based on the support of 1033 Glioma tumor samples, 1092 meningioma tumor samples, 1158 pituitary tumor samples, and 1286 non-tumor samples.

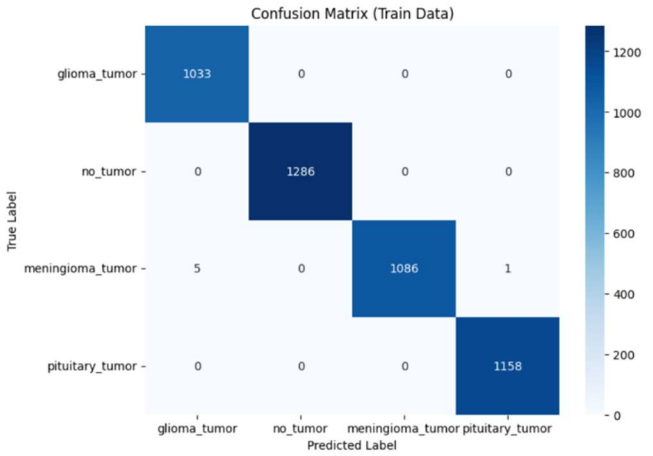

Figure 10. Confusion Matrix for Training Data for 4569 MRI Images.

The classification report is generated from the Confusion matrix, as shown in Figure 11. Our Training classification report shows that the proposed model has 100% accurate precision, 100% accurate Recall, and 100% accurate F1-score for glioma tumor samples. It has 100% accurate precision, 100% accurate Recall, and 100% accurate F1-score for non-tumor image samples. It has 100% accurate precision, 100% accurate Recall, and 100% accurate F1-score for Pituitary tumor samples. the proposed model has 100% accurate precision, 100% accurate Recall, and 100% accurate F1-score for glioma tumor samples. It achieves 100% accuracy in precision, 99% accuracy in recall, and 100% accuracy in F1-score for meningioma tumor samples. It also shows a 100% value of the macro average and a 100% value of the weighted average for 4569 support samples. The Multiclass ROC curve is framed between the TPR and the FPR positive rate in Figure 12. In the AUC-ROC curve, AUC curve means Area Under the Curve, and ROC means Receiver Operating Characteristics. AUC-ROC Curve is used to measure the performance of the model based on its TPR and FPR. The value of the AUC-ROC curve lies between 0 to 1, and the closer it is to 1, the higher the classification performance of the model. If its value is 1, it means that the model can do 100% accurate classification, but

if its value is 50%, then we cannot trust the model at all because in this case, it is classifying randomly. In our AUC-ROC curve, we can see that its value is almost equal to 1, which means our model can accurately assess

Classification Report (Train Data):

	precision	recall	f1-score	support
glioma_tumor	1.00	1.00	1.00	1033
no_tumor	1.00	1.00	1.00	1286
meningioma_tumor	1.00	0.99	1.00	1092
pituitary_tumor	1.00	1.00	1.00	1158
accuracy			1.00	4569
macro avg	1.00	1.00	1.00	4569
weighted avg	1.00	1.00	1.00	4569

Figure 11. Training Classification Report based on Confusion Matrix

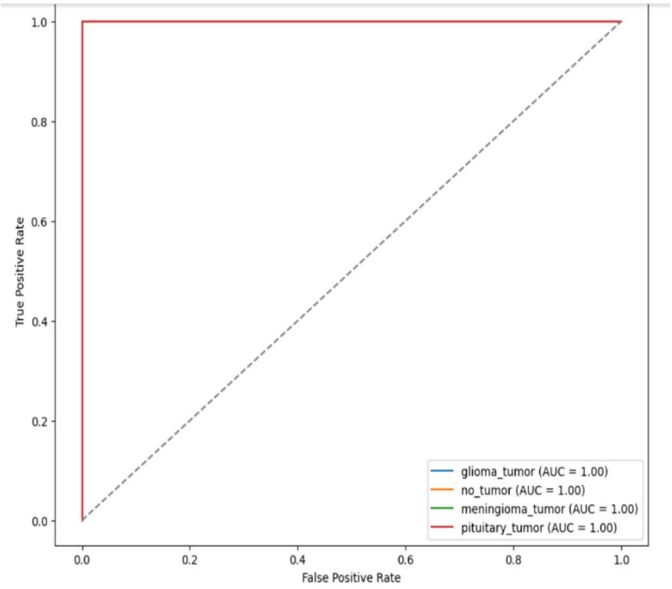

Figure 12. Training Data Multiclass AUC-ROC Curve.

The Loss Curve Graph, plotted between Loss and number of Epochs, is plotted in Figure 13. The graph between Training and Validation Accuracy is framed in Figure 14.

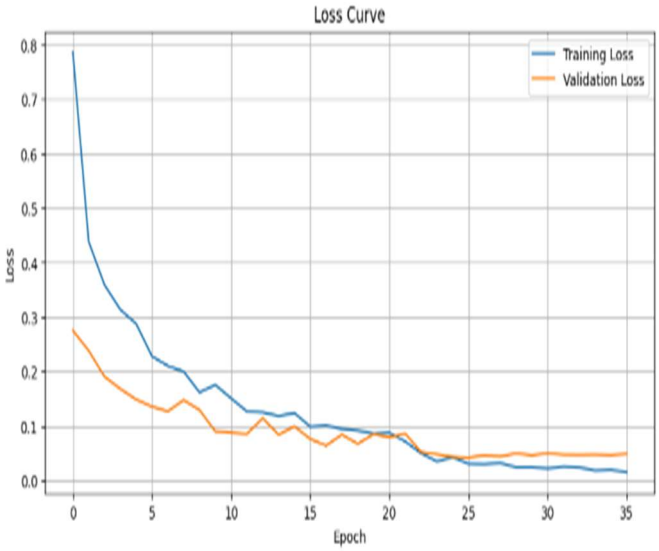

Figure 13. Training and Validation Loss Representation.

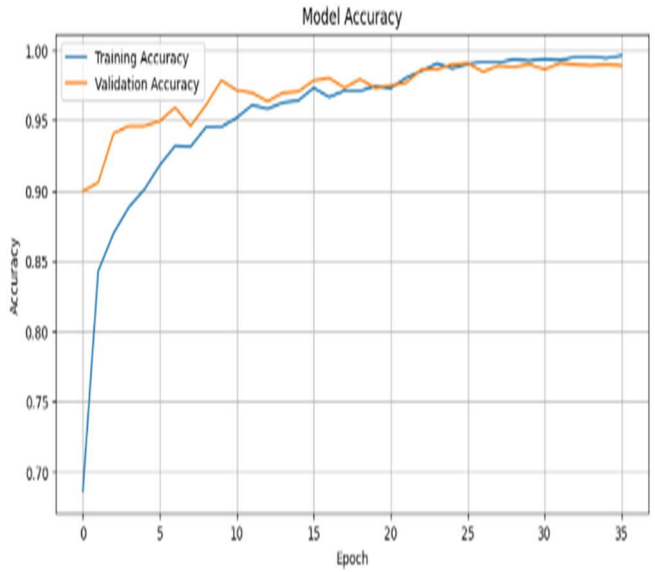

Figure 14. Training and Validation Accuracy Representation.

B. TESTING PHASE

After completion of training and validation, testing is achieved on the 1311 training samples taken from the same dataset. The Testing valuation confusion matrix is represented in Figure 15. The confusion matrix is generated by considering the support of 300 Glioma tumor specimens, 306 meningioma tumor specimens, 300 pituitary tumor specimens, and 405 no-tumor specimens.

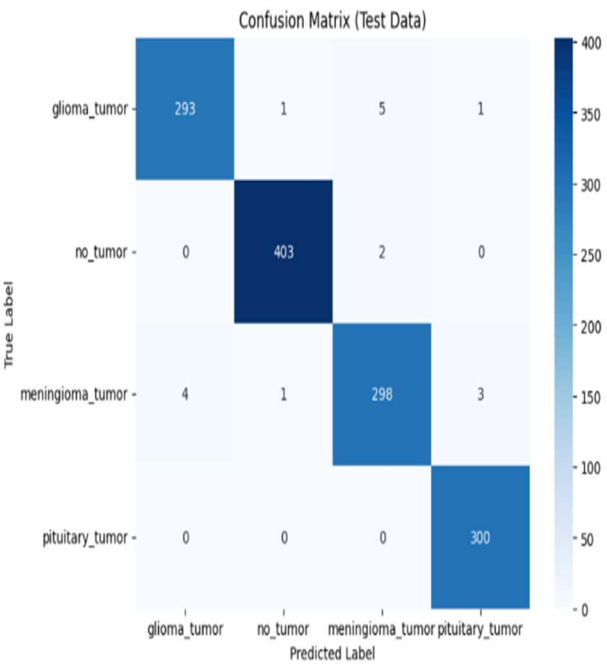

Figure 15. Confusion Matrix for Testing Data.

The classification report is produced from the Confusion matrix represented in Figure 16. Our Testing classification report shows that the proposed model has 99% precision, 98% Recall, and 98% F1-score for 300 support samples of Glioma tumors. It has 100% precision, 100% Recall, and 100% F1-score for 405 support samples of no tumors. It has 98% precision, 97% Recall, and 98% F1-score for 306 support samples of Meningioma tumor. It has 99% precision, 100%

Recall, and 99% F1-score for 300 support samples of Pituitary tumors. Our Model achieved 99% Accuracy on a total of 1311 support samples. It has a value of 99% for macro (avg) and weighted (avg) for Precision, Recall, and F1-score on 1311 support samples.

Classification Report (Test Data):

	precision	recall	f1-score	support
glioma_tumor	0.99	0.98	0.98	300
no_tumor	1.00	1.00	1.00	405
meningioma_tumor	0.98	0.97	0.98	306
pituitary_tumor	0.99	1.00	0.99	300
accuracy			0.99	1311
macro avg	0.99	0.99	0.99	1311
weighted avg	0.99	0.99	0.99	1311

Figure 16. Classification Report based on Testing Confusion Matrix.

We have tested our model for different labels as shown in Figure 17. The results show that the proposed model is correct in predicting the case of multiclass classification.

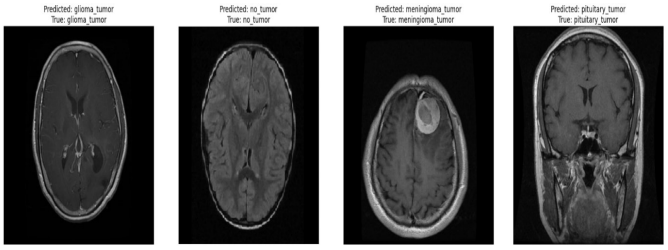

Figure 17. Model Showing Accurate Prediction.

VI. MODEL PERFORMANCE AND COMPARATIVE ANALYSIS

Comparative analysis was obtained by considering various benchmarks. Initially, we have compared our proposed model's training and testing results based on various performance benchmarks, we have calculated. In Table 1, we have compared based on the final values of these parameters, and as one can see, there is not much difference between the values of parameters in both training and testing, proving how accurately our model is working. In Table 2 we have compared based on individually the types of brain tumors and non-tumor values for all parameters and as one can see in the case of No tumor images our model is 100% accurately predicting as all the performance parameters are 100%, while for other cases, i.e.; tumor classes it is 99% predicting accurately (see weighted average and macro average).

Table 1. Comparison of Testing and Training results obtained for the proposed model regarding various performance benchmarks

Metric	Training Values Obtained	Testing Values Obtained
Accuracy	99.9	99.1
Precision	99.9	99.0
Recall (Sensitivity)	99.9	99.0
F-1 Score	99.9	99.0
Average Sensitivity	99.9	99.0
Average Specificity	100.0	99.6

Table 2. Multiclass Comparison of Testing and Training results obtained for the proposed model regarding various performance benchmarks

Class	Parameter	Precision	Recall	F-1 Score	Support
Glioma-Tumor	Training	100.0	100.0	100.0	1033
	Testing	99.0	98.0	98.0	300
No-Tumor	Training	100.0	100.0	100.0	1286
	Testing	100.0	100.0	100.0	405
Meningioma Tumor	Training	100.0	99.0	100.0	1092
	Testing	98.0	97.0	98.0	306
Pituitary Tumor	Training	100.0	100.0	100.0	1158
	Testing	97.0	100.0	99.0	300
Weighted Average	Training	100.0	100.0	100.0	4569
	Testing	99.0	99.0	99.0	1311
Macro Average	Training	100.0	100.0	100.0	4569
	Testing	99.0	99.0	99.0	1311

Now comparison is achieved with the existing approaches based on the types of tumor and parameters taken, including support values. In the case of a Glioma tumor (Table 3), our model has better precision (99%) and Accuracy (99%) with maximum support values. Others have less or equal support value as compared to the proposed model. In the case of a Meningioma tumor (Table 4), our model dominates as it has all the performance parameters better than others. In the case of a Pituitary tumor (Table 5), our model has better recall (100%) and Accuracy (99%) with maximum support values. In the case of a No tumor (Table 6), our model again dominates as it has all the performance parameters better than others with maximum support values.

Table 3. Multiclass Comparison of Testing Results (Glioma)

#	Year	Precision	Recall (Sensitivity)	F1-Score	Accuracy	Support
[36]	2021	93.4	94.4	-	97.85	190
[37]	2024	**99.0**	96.0	97.0	98.20	127
[38]	2024	**99.0**	94.0	96.0	98.0	**300**
[39]	2023	**99.0**	98.67	**99.19**	99.0	286
[40]	2023	96.0	**99.0**	98.0	98.0	266
Proposed		**99.0**	98.0	98.0	**99.1**	**300**

Table 4. Multiclass Comparison of Testing Results (Meningioma)

#	Year	Precision	Recall (Sensitivity)	F1-Score	Accuracy	Support
[36]	2021	92.3	92.4	-	97.6	**490**
[37]	2024	97.0	95.0	96.0	98.20	123
[38]	2024	94.0	96.0	95.0	98.0	405
[39]	2023	96.55	96.54	96.55	99.0	142
[40]	2023	97.0	93.0	95.0	98.0	152
Proposed		**98.0**	**97.0**	**98.0**	**99.1**	306

Table 5. Multiclass Comparison of Testing Results (Pituitary)

#	Year	Precision	Recall (Sensitivity)	F1-Score	Accuracy	Support
[36]	2021	90.9	88.0	-	96.96	140
[37]	2024	96.0	99.0	97.0	98.20	126
[38]	2024	97.0	99.0	98.0	98.0	**300**
[39]	2023	97.42	98.45	97.93	99.0	186
[40]	2023	**100.0**	99.0	**100.0**	98.0	195
Proposed		99.0	**100.0**	99.0	**99.1**	**300**

Table 6. Multiclass Comparison of Testing Results (No Tumor)

#	Year	Precision	Recall (Sensitivity)	F1-Score	Accuracy	Support
[36]	2021	88.0	92.1	-	95.44	170
[37]	2024	97.0	99.0	98.0	98.20	68
[38]	2024	**100.0**	**100.0**	**100.0**	98.0	306
Proposed		**100.0**	**100.0**	**100.0**	**99.1**	**405**

We have also compared the performance results of the developed model with other existing models based on the various benchmarks (Table 7). We had previously experimented with EfficientNet and ResNet on the same dataset and measured their performance using popular parameters. The results of which are also shown in Table 7. However, the results obtained by EfficientNet and ResNet individually were not that influential. Therefore, we combined both these networks to utilize their best features and developed a hybrid model whose performance is better than the individual performances of both these models. Table 7 is used to show the overall performance of our proposed model. This table contains the overall maximum accuracy, Recall, F1-score, and Precision achieved by our proposed model and the comparative analysis of the proposed model with the other existing models on the basis of these performance parameters, to represent the status of our model. Our model is giving excellent results as compared to all the other models, on different performance parameters. We have also shown the performance of our model in cases when we implemented it with ResNet and EfficientNet individually, and our hybrid model performed better in all aspects.

Table 7. Comparison with Existing Approaches Based on Performance Parameters

#	Year	Accuracy (%)	Recall (%)	F1-Score	Precision
[27]	2024	96.03	96.03	96.0	96.02
[28]	2024	96.0	93.00	93.0	93.0
[41]	2024	98.99	**99.16**	96.52	96.52
[42]	2024	92.0	92.0	92.0	92.0
[43]	2023	96.47	95.0	-	-
[44]	2022	98.91	99.0	98.57	98.28
[45]	2024	98.0	98.0	98.0	98.0
[46]	2023	93.3	91.19	-	-
[47]	2022	93.74	92.1	92.0	92.0
[48]	2023	96.68	98.0	97.0	97.0
[37]	2024	98.20	97.0	97.0	97.0
[38]	2024	98	99.0	97.0	97.0
[39]	2024	99.0	**99.13**	98.73	98.73
[40]	2023	97.7	98.0	98.0	98.0
ResNet		**95.88**	98.24	**96.99**	**97.75**
EfficientNet		**97.73**	96.55	**98.75**	**96.95**
Proposed		**99.1**	99.0	**99.0**	**99.0**

Our model performs better in 3 out of 4 parameters: Accuracy, F1 Score, and Precision, while in the remaining 1 parameter, Recall, there is only a slight difference, which is only in a few decimal values. These comparative results show that our model is an accurate model that can efficiently classify different types of tumor images (multi-class tumor images) and non-tumor images, and gives accurate results. Generally, CNNs are extremely cost-efficient as their computational cost is very low. Hence, they are used a lot in the case of image segmentation. Here, our purpose was to develop a lightweight model, so we have used CNNs. Generally, the results of CNNs are very good and fast with small datasets. However, currently, some novel techniques like vision transformers are also being used. These transformers have the potential to give good performance when trained with large datasets. However, their computational cost is high due to consuming more resources and time in the training process, and their data dependency becomes high when trained with smaller datasets, and also requires a lot of data augmentation techniques. However, their performance in solving complex problems with large datasets is higher than CNNS in many ways. In the future, we will try to make our model even more efficient by further enhancing our datasets and using these transfers.

VI. CONCLUSIONS

Brain tumors can attack people of any age, whether old, young, or child. If a brain tumor is detected early, it is possible to treat it, otherwise, later it turns into cancer, which is difficult to cure and the chances of survival of the patient are very low. Deep Learning technology and its innovative derivative transfer learning play a vital role in the medical field due to its important characteristics like pure and faster measurement, efficient calculation, and accurate results. We have introduced a new and innovative transfer learning model in which two popular convolutional Networks have been combined so that our hybrid model contains their best features. The first CNN we have taken is EfficientNetV2B3, which has 384 layers and is used for faster and more accurate processing. The second CNN is ResNetV2, which has 564 layers and is a residual neural network used to access deep features. We have fine-tuned the last 30 layers of both CNNs and then added 16 custom layers. The proposed model achieved maximum accuracy value, maximum recall value, maximum precision value,

maximum F-1 score value, and average specificity value of 99.99%, 99.99%, 99.99%, 99.99%, and 100% respectively during training. While during testing it achieved maximum accuracy value, maximum recall value, maximum precision value, maximum F-1 score value, and average specificity value of 99.1%, 99.00%, 99.00%, 99.00%, and 99.6% respectively. In the case of comparing multi-level classification (Glioma Tumor, Meningioma Tumor, Pituitary Tumor, and No Tumor), the proposed model achieved a maximum accuracy value of 100%, maximum recall value of 100%, maximum precision value of 100%, and maximum F-1 score value of 100% for all four classes, during training. While during testing it achieved maximum accuracy value, maximum recall value, maximum precision value, and maximum F-1 score value of 99.1% (all classes), 100.00% (Pituitary and No tumor classes), 100.00% (No Tumor class), and 100.00% (No Tumor Class), respectively. We have also compared this model with recent existing models developed to solve the same issue. These comparisons show that this model obtained ultimate results in computing accurate results, F-1 score calculation, and precision level compared to all the other recently existing models. In this model, we have used publicly available datasets collected from trusted sources, and to reduce the computational cost of the model, we have used Google Colab Pro+, through which we have achieved faster GPUs, faster RAM, and faster processing at a very low cost. Also, the accuracy of our model is 99%, which shows that this is a highly accurate model and the chance of error in it is only 1%, hence, it can be used very efficiently in clinical applications.

In the future, we will make further improvements in our model using some other advanced augmentation techniques, such as MixUp, CutMix, or RandAugment come under the category of mix augmentations, to extend its performance to another level. We will also try to extend our model to larger datasets and will use some other advanced techniques, such as Swin Transformer or Vision Transformers, and increase the number of performance parameters, such as prevalence, ERR Rate, so that their performance can be enhanced and analyzed at a more detailed level.

References

[1] N. Simhadri and T.N.V.R Swami, "Awareness among teaching on AI and ML applications based on fuzzy in education sector at USA," *Soft Comput* (2023). https://doi.org/10.1007/s00500-023-08329-z.

[2] S. Chen, J. Yu, S. Chamouni, *et al.*, "Integrating machine learning and artificial intelligence in life-course epidemiology: pathways to innovative public health solutions," *BMC Med*, vol. 22, 354, 2024. https://doi.org/10.1186/s12916-024-03566-x.

[3] M. Rana, M. Bhushan, "Machine learning and deep learning approach for medical image analysis: Diagnosis to detection," *Multimed Tools Appl*, vol. 82, pp. 26731–26769, 2023. https://doi.org/10.1007/s11042-022-14305-w.

[4] G. M. Rao, D. Ramesh, V. Sharma, *et al.*, "AttGRU-HMSI: enhancing heart disease diagnosis using hybrid deep learning approach," *Sci Rep*, vol. 14, 7833, 2024. https://doi.org/10.1038/s41598-024-56931-4.

[5] B. F. Wee, S. Sivakumar, K. H. Lim, *et al.*, "Diabetes detection based on machine learning and deep learning approaches," *Multimed Tools Appl*, vol. 83, pp. 24153–24185, 2024. https://doi.org/10.1007/s11042-023-16407-5.

[6] Ö.F. Akmeşe, "Data privacy-aware machine learning approach in pancreatic cancer diagnosis," *BMC Med Inform Decis Mak*, vol. 24, 248, 2024. https://doi.org/10.1186/s12911-024-02657-2.

[7] K. K. Joshi, K. Gupta, & J. Agrawal, "An efficient transfer learning approach for prediction and classification of SARS – COVID-19," *Multimed Tools Appl*, vol. 83, pp. 39435–39457, 2024. https://doi.org/10.1007/s11042-023-17086-y.

[8] Q. Xiang, D. Li, Z. Hu, *et al.*, "Quantum classical hybrid convolutional neural networks for breast cancer diagnosis," *Sci Rep*, vol. 14, 24699 (2024). https://doi.org/10.1038/s41598-024-74778-7.

[9] L. Van Dieren, J. Z. Amar, N. Geurs, *et al.*, "Unveiling the power of convolutional neural networks in melanoma diagnosis," *Eur J Dermatol*, vol. 33, pp. 495–505, 2023. https://doi.org/10.1684/ejd.2023.4559.

[10] F. Hoseini, S. Shamlou, & M. Ahmadi-Gharehtoragh, "Segmentation of MR images for brain tumor detection using autoencoder neural network," *Discov Artif Intell*, vol. 4, 71, 2024. https://doi.org/10.1007/s44163-024-00180-x.

[11] K. Kumar, K. Jyoti, & K. Kumar, "Machine learning for brain tumor classification: evaluating feature extraction and algorithm efficiency," *Discov Artif Intell*, vol. 4, 112, 2024. https://doi.org/10.1007/s44163-024-00214-4.

[12] M. Ahmed, M. Nadeem, U. B. Shahzad, *et al.*, "A comprehensive approach to lateral ventricular tumor resection: Techniques, technologies, and outcomes," *Neurosurg Rev*, vol. 47, 489, 2024. https://doi.org/10.1007/s10143-024-02745-x.

[13] N. Elazab, W. Gab Allah, & M. Elmogy, "Computer-aided diagnosis system for grading brain tumor using histopathology images based on color and texture features," *BMC Med Imaging*, vol. 24, 177, 2024. https://doi.org/10.1186/s12880-024-01355-9.

[14] M. Reichenbach, S. Richter, R. Galli, *et al.*, "Clinical confocal laser endomicroscopy for imaging of autofluorescence signals of human brain tumors and non-tumor brain," *J Cancer Res Clin Oncol*, vol. 151, 19, 2025. https://doi.org/10.1007/s00432-024-06052-2.

[15] Z. Mansur, J. Talukdar, T. P. Singh, *et al.*, "Deep learning-based brain tumor image analysis for segmentation," *SN COMPUT. SCI.*, vol. 6, 42, 2025. https://doi.org/10.1007/s42979-024-03558-x.

[16] R. Ahsan, I. Shahzadi, F. Najeeb, *et al.*, "Brain tumor detection and segmentation using deep learning," *Magn Reson Mater Phy*, vol. 38, pp. 13-22, 2024. https://doi.org/10.1007/s10334-024-01203-5.

[17] S. Ganapathy, V. Thoidingjam, & A. Sen, "A brain tumor prediction system for detecting the tumor disease using mini batch K-Means clustering and CNN," *Multimed Tools Appl*, vol. 83, pp. 83053–83091, 2024. https://doi.org/10.1007/s11042-024-18790-z.

[18] D. Black, D. Byrne, A. Walke, *et al.*, "Towards machine learning-based quantitative hyperspectral image guidance for brain tumor resection," *Commun Med*, vol. **4**, 131, 2024. https://doi.org/10.1038/s43856-024-00562-3.

[19] Chakrapani, S. Kumar, S. Semantic segmentation of brain tumor images using attention-based residual light u-net model. *Multimed Tools Appl*, vol. 84, pp. 7425-7441, 2024. https://doi.org/10.1007/s11042-024-19224-6.

[20] S. K. Natarajan, S. J.ayanthi, S. K. Mathivanan, *et al.*, "Exploring fetal brain tumor glioblastoma symptom verification with self organizing maps and vulnerability data analysis," *Sci Rep*, vol. 14, 8738, 2024. https://doi.org/10.1038/s41598-024-59111-6.

[21] T. K. Dutta, D. R. Nayak, & R. B. Pachori, "GT-Net: global transformer network for multiclass brain tumor classification using MR images," *Biomed. Eng. Lett.*, vol. 14, pp. 1069–1077, 2024. https://doi.org/10.1007/s13534-024-00393-0.

[22] C. Tao, D. Gu, R. Huang, et al., "Hippocampus segmentation after brain tumor resection via postoperative region synthesis," *BMC Med Imaging*, vol. 23, 142, 2023. https://doi.org/10.1186/s12880-023-01087-2.

[23] Y. Abdelrahman Ali, T. Kamani, S. K. Patel, *et al.*, "Design and investigation of machine learning–optimized surface plasmon resonance biosensor for early brain tumor detection," *Plasmonics*, 2024. https://doi.org/10.1007/s11468-024-02635-4.

[24] A. Kaur, Y. Singh, & B. Chinagundi, "ResUNet + + : a comprehensive improved UNet + + framework for volumetric semantic segmentation of brain tumor MR images," *Evolving Systems*, vol. 15, pp. 1567–1585, 2024. https://doi.org/10.1007/s12530-024-09579-4.

[25] S. Poornam, J.J.R. Angelina, "BrainNeuroNet: advancing brain tumor detection with hierarchical transformers and multiscale attention," *Int. J. Inf. Tecnol.*, vol. 16, pp. 4749–4756, 2024. https://doi.org/10.1007/s41870-024-02216-y.

[26] M. M. Gomaa, A. G. Zain elabdeen, A. Elnashar, *et al.*, "Brain tumor X-ray images enhancement and classification using anisotropic diffusion filter and transfer learning models," *Int. J. Inf. Tecnol.*, vol. 16, pp. 3771–3779, 2024. https://doi.org/10.1007/s41870-024-01830-0.

[27] M. Basthikodi, M. Chaithrashree, B. M. Ahamed Shafeeq, *et al.*, "Enhancing multiclass brain tumor diagnosis using SVM and innovative feature extraction techniques," *Sci Rep*, vol. 14, 26023, 2024. https://doi.org/10.1038/s41598-024-77243-7.

[28] A. H. Tiple, A. B. Kakade, "Modified mask R-CNN with KNN algorithm based segmentation and classification for prediction of brain tumor

types," *Optoelectron. Instrument. Proc.*, vol. 60, pp. 11–30, 2024. https://doi.org/10.3103/S8756699024700146.
[29] B. Swathi, S. S. Kolisetty, G.V. Sivanarayana, *et al.*, "Efficientnetv2-RegNet: an effective deep learning framework for secure SDN based IOT network," *Cluster Comput*, vol. 27, pp. 10653–10670, 2024. https://doi.org/10.1007/s10586-024-04498-0.
[30] P. V. Sabique, G. Pasupathy, S. Kalaimagal, *et al.*, "A stereovision-based approach for retrieving variable force feedback in robotic-assisted surgery using modified inception ResNet V2 networks," *J Intell Robot Syst*, vol. 110, 81, 2024. https://doi.org/10.1007/s10846-024-02100-8.
[31] K. Faber, D. Zurek, M. Pietron, *et al.*, "From MNIST to ImageNet and back: benchmarking continual curriculum learning," *Mach Learn*, vol. 113, pp. 8137–8164, 2024. https://doi.org/10.1007/s10994-024-06524-z.
[32] N. Boudouh, B. Mokhtari, & S. Foufou, "Enhancing deep learning image classification using data augmentation and genetic algorithm-based optimization," *Int J Multimed Info Retr*, vol. 13, 36, 2024. https://doi.org/10.1007/s13735-024-00345-5.
[33] K. Alomar, H. I. Aysel, X. Cai, "Data augmentation in classification and segmentation: A survey and new strategies," *J. Imaging*, vol. 9, 46, 2023. https://doi.org/10.3390/jimaging9020046.
[34] V. Werner de Vargas, J. A. Schneider Aranda, R. dos Santos Costa, *et al.*, "Imbalanced data preprocessing techniques for machine learning: a systematic mapping study," *Knowl Inf Syst*, vol. 65, pp. 31–57, 2023. https://doi.org/10.1007/s10115-022-01772-8.
[35] D.J.J. Seeli, K.K. Thanammal, "A comparative review and analysis of medical image encryption and compression techniques," *Multimed Tools Appl*, 2024. https://doi.org/10.1007/s11042-024-18745-4.
[36] E. Irmak, "Multi-classification of brain tumor MRI images using deep convolutional neural network with fully optimized framework," *Iran J Sci Technol Trans Electr Eng*, vol. 45, pp. 1015–1036, 2021. https://doi.org/10.1007/s40998-021-00426-9.
[37] S M. Rasa et al., "Brain tumor classification using fine-tuned transfer learning models on magnetic resonance imaging (MRI) images," *Digital Health*, 2024. https://doi.org/10.1177/20552076241286140.
[38] E. Albalawi, T. R. Manesh, A. Thakur, *et al.*, "Integrated approach of federated learning with transfer learning for classification and diagnosis of brain tumor," *BMC Med Imaging*, vol. 24, 110, 2024. https://doi.org/10.1186/s12880-024-01261-0.
[39] B. Babu Vimala, S. Srinivasan, S. K. Mathivanan, *et al.*, "Detection and classification of brain tumor using hybrid deep learning models," *Sci Rep*, vol. 13, 23029, 2023. https://doi.org/10.1038/s41598-023-50505-6.
[40] K. V. Archana, and G. Komarasamy, "A novel deep learning-based brain tumor detection using the Bagging ensemble with K-nearest neighbor," *Journal of Intelligent Systems*, vol. 32, no. 1, 20220206, 2023. https://doi.org/10.1515/jisys-2022-0206.
[41] M. Yurtsever, Y. Atay, B. Arslan, *et al.*, "Development of brain tumor radiogenomic classification using GAN-based augmentation of MRI slices in the newly released gazi brains dataset," *BMC Med Inform Decis Mak*, vol. 24, 285, 2024. https://doi.org/10.1186/s12911-024-02699-6.
[42] G. Bogacsovics, B. Harangi, & A. Hajdu, "Developing diverse ensemble architectures for automatic brain tumor classification," *Multimed Tools Appl*, 2024. https://doi.org/10.1007/s11042-024-19657-z.
[43] S. Saeedi, S. Rezayi, H. Keshavarz, *et al.*, "MRI-based brain tumor detection using convolutional deep learning methods and chosen machine learning techniques," *BMC Med Inform Decis Mak*, vol. 23, 16, 2023. https://doi.org/10.1186/s12911-023-02114-6.
[44] N. Ullah, J.A. Khan, M.S. Khan, W. Khan, I. Hassan, M. Obayya, N. Negm, A.S. Salama, "An effective approach to detect and identify brain tumors using transfer learning," *Appl. Sci.*, vol. 12, 5645, 2022. https://doi.org/10.3390/app12115645.
[45] M.Z. Khaliki, M.S. Başarslan, "Brain tumor detection from images and comparison with transfer learning methods and 3-layer CNN," *Sci Rep*, vol. 14, 2664, 2024. https://doi.org/10.1038/s41598-024-52823-9.
[46] M.I. Mahmud, M. Mamun, A. Abdelgawad, "A deep analysis of brain tumor detection from MR images using deep learning networks," *Algorithms*, vol. 16, 176, 2023. https://doi.org/10.3390/a16040176.
[47] A. Alshammari, "Construction of VGG16 convolution neural network (VGG16_CNN) classifier with NestNet-based segmentation paradigm for brain metastasis classification," *Sensors*, vol. 22, 8076, 2022. https://doi.org/10.3390/s22208076.
[48] M. Islam, M.T. Reza, M. Kaosar, *et al.*, "Effectiveness of federated learning and CNN ensemble architectures for identifying brain tumors using MRI images," *Neural Process Lett*, vol. 55, pp. 3779–3809, 2023. https://doi.org/10.1007/s11063-022-11014-1.

***NEELAM KHEMARIYA** Presently pursuing PhD in Computer Science Engineering from Mangalayatan University, Aligarh, Uttar Pradesh. She has done her Master of Technology from Rajasthan Technical University, Kota, Rajasthan in Software Engineering (Gold Medalist) and her Bachelor of Engineering from Rajiv Gandhi Proudyogiki Vishwavidyalaya, Bhopal, Madhya Pradesh in Computer Science and Engineering. She has published more than 30 papers in Reputed International Journals and Conferences. She is a reviewer of many conferences. She has two patent publications and edited one international book chapter. She has more than 17 years of academic experience. She taught various subjects including Operating Systems, Computer Networks, and Machine Learning. Her areas of interest are Deep Learning, Transfer Learning, and Medical Imaging.*

***SUMIT SINGH SONKER** is an Assistant Professor in the Department of Computer Engineering & Application at the Institute of Engineering and Technology at Mangalayatan University, Uttar Pradesh. Further Assistant Professor Sumit Sonker guided Ph.D. scholars. Prof. Sumit Sonker completed her post-graduation in MCA from VINAYAKA MISSIONS University, Salem, and a Ph.D. in Computer Science and engineering from CMJ University Shillong. His Doctoral Research was on "Study and Analysis of Software Testing Techniques to Develop a Specialized Testing Tool". In addition, has been involved in the NGO – Gurukul Jyoti Welfare Society, Providing free education to students in terms of skill development and self-employment courses. He has published many Articles in national and international Journals. His research areas are Management Information Systems (MIS), Communication and Information system, Cloud Computing, Social Deep Learning, Machine Learning, and Image Processing.*

***JAVED WASIM** Presently working as an Associate Professor and Head of the Department, of Computer Engineering, at Mangalayatan University. He has obtained PhD in Computer Science Engineering. He has published several quality papers in Reputed International Journals and Conferences. He is an active member of various international and national educational bodies. He taught various subjects including Machine Learning, Image Processing, and Deep Learning. His areas of interest are Deep Learning, Machine Learning, and Image Processing.*